Hyperfine Interact
DOI 10.1007/s10751-013-1007-2

^{57}Fe Mössbauer study of a secondary phase in $FeSe_{1-x}$ with a large quadrupole splitting

A. Sklyarova · J. Lindén · G. C. Tewari · E.-L. Rautama · M. Karppinen

Abstract We have studied the hyperfine interactions in samples belonging to the Fe-Se system. Several samples with various concentrations of selenium were synthesized and investigated. The objective was to find synthesis conditions increasing the concentration of a secondary Fe-Se phase with a rather large quadrupole splitting of ∼1.7 mm/s. At $T_m \approx 104$ K this secondary phase undergoes a magnetic ordering.

Keywords ^{57}Fe Mössbauer spectroscopy · Chalcogenide superconductivity · Magnetic properties

1 Introduction

FeSe forms in a simple structure that exhibits superconducting properties at an optimal 1:1 stoichiometric composition of Fe and Se [1]. The transition temperature of this material

Proceedings of the 32nd International Conference on the Applications of the Mössbauer Effect (ICAME 2013) held in Opatija, Croatia, 1–6 September 2013

A. Sklyarova (✉) · J. Lindén
Physics Department, Åbo Akademi University, FI-20500 Turku Finland
e-mail: asklyaro@abo.fi

J. Lindén
e-mail: jlinden@abo.fi

A. Sklyarova
Faculty of Physics, Lappeenranta University of Technology, Box 20, 53851 Lappeenranta, Finland

A. Sklyarova
Faculty of Physics, St. Petersburg State University, Ulyanovskaya Str. 1, Petrodvorets, St. Petersburg, 198504 Russia

G. C. Tewari · E.-L. Rautama · M. Karppinen
Department of Chemistry, Aalto University, FI-00076 Aalto, Finland

Published online: 23 January 2014

is low (∼8 K) but it can be raised e. g. by applying an external pressure [2, 3]. During the synthesis mixtures of Fe and Se can form various phases: α-FeSe, β-FeSe and γ-FeSe [1, 4]. The composition of the phases obtained and their structures (tetragonal, hexagonal NiAs-type) depend on the selenium content and the temperature of the synthesis [5]. Superconductivity in this compound can exists only in the tetragonal phase below $T_c \approx 8$ K [1, 5].

All phases which FeSe can form show a magnetically ordered structure, except the phase with a tetragonal structure, which at room temperature resides in a paramagnetic state. Upon cooling this material undergoes a tetragonal-to-orthorhombic structural transition at ∼90 K. The temperature of this structural transition depends on the exact stoichiometry of the material. Under an applied hydrostatic pressure a magnetic ordering of non-stoichiometric superconducting $FeSe_{1-x}$ ($x = 0.02 - 0.06$) has been reported [6, 7].

Due to paramagnetism ^{57}Fe Mössbauer spectra of pure FeSe with tetragonal structure consist of a single doublet at room temperature. In $FeSe_{0.82}$ prepared by solid-state reaction by quenching from 650 °C to room temperature an additional paramagnetic doublet in the Mössbauer spectrum was observed [8]. This doublet, characterized by a high quadrupole splitting of ∼1.7 mm/s, was assigned to an impurity phase but its origin was not known. This doublet was also observed by another group and two possible origins of its were discussed but the exact nature of this impurity phase was not determined [9].

The purpose of this work was to prepare and investigate this secondary phase that appears in compounds with a selenium deficiency. Several samples with various concentrations of selenium were synthesized and investigated by Mössbauer spectroscopy. Optimizing the conditions for the secondary phase required some efforts because the exact preparation route was not known from the literature.

2 Experimental

It was found that in our samples the second paramagnetic doublet becomes visible only after a second synthesis step. Two different temperature were used for samples preparation: 650 °C [8, 10] and 750 °C.

Two series of samples with stoichiometries of $FeSe_{0.6}$, $FeSe_{0.75}$, $FeSe_{0.82}$, and $FeSe_{0.9}$ were prepared at 750 °C and investigated. Stoichiometric ratios of iron (99.99 %) and selenium (99.99 %) powders were mixed, sealed in evacuated quartz tubes and annealed at 750 °C for 20 h and quenched into cold water. The obtained samples were denoted series I. Thereafter, a portion of the powders of series I were reground in a mortar, pressed into pellets and sintered again at the same synthesis conditions. After 20 h the samples were quickly taken out of the furnace and quenched into cold water. These samples were denoted series II.

The phase and structure determination were carried out by X-ray powder diffraction (PanAnalytical X'Pert Pro MPD diffractometer). ^{57}Fe Mössbauer spectra were recorded with Doppler velocities of 8.04 mm/s and 2.53 mm/s in transmission geometry in the temperature interval 77 − 300 K using an Oxford CF506 continuous-flow cryostat and a year-old Cyclotron Co, ^{57}Co:Rh source. The spectra were fitted using the following parameters: line width (Γ) was fixed for all components to be equal excluding the 2^{nd} (M) component (the secondary component which undergoes a magnetic ordering and exhibits a rather broad

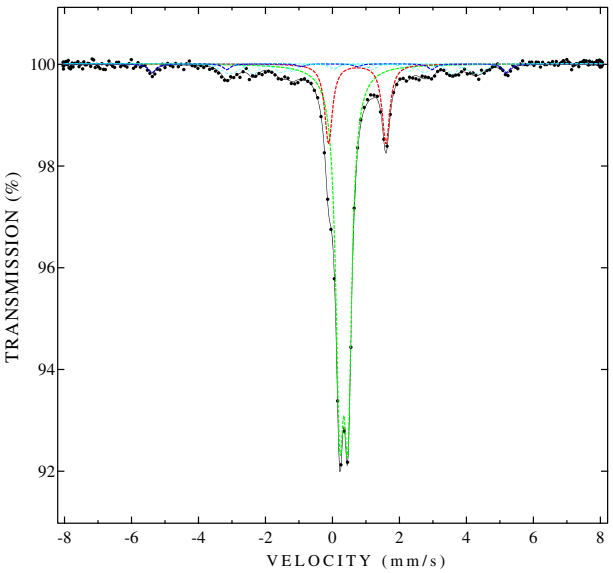

Fig. 1 High-velocity Mössbauer spectrum of the series II $FeSe_{0.9}$ sample recorded at 300 K. Doublets due to the main phase, the secondary phase, and sextets due to elementary iron, and Fe_7Se_8 are drawn in *green*, *red*, *blue*, and *cyan*, respectively

sextet), quadrupole splitting ($QS = eQV_{zz}/2$), isomer shift (δ), component intensities (I), and magnetic hyperfine field (B_{eff}) for magnetically-split components. Isomer shift values are quoted relative to α-Fe at room temperature.

3 Results and discussion

In Fig. 1 a high-velocity Mössbauer spectrum for $FeSe_{0.9}$ of series II is shown. A large portion of a secondary Fe phase is seen with its characteristic large quadrupole splitting. Certain amounts of elementary iron (around 3 % for $FeSe_{0.9}$) were observed. The iron impurity was found in all recorded spectra, most intense in the compound with lowest Se content: 33 % Fe in FeSe0.6 (see Table 1 presented below).

Experimental XRD data for samples $FeSe_{0.6}$ $FeSe_{0.9}$ of series I and II were fitted using the Rietveld method and the program FullProf [11]. The patterns revealed the presence of the FeSe main phase, an unknown Fe-Se phase, Fe_7Se_8 and elementary Fe. The Bragg peaks due to the unknown phase are significantly sharper than the ones coming from the main FeSe phase and the observed Fe_7Se_8 phase. This is a strong indicator that these unidentified reflections are not related to these compositions e.g. in a way of distortion. Despite of a careful and extensive search of the diffraction database, including possible reaction with silica, no match was found for the unaccounted reflections in the XRD pattern. As the heat-treatments clearly increased the intensities of all these unidentified reflections, we suspect that they are coming from one phase. To provide some information of this, we have attempted to find its unit cell by indexing all the reflections that cannot be explained by β-

Table 1 Parameters of the $FeSe_{1-x}$ Mössbauer spectra at RT and around T_m. For the secondary component P denotes paramagnetic and M magnetic

Origin	T, K	Γ, mm/s	δ, mm/s	QS, mm/s	B_{eff}, T	A^1, %	T_m, K
$FeSe_{0.6}$							
FeSe	298	0.276(5)	0.458(5)	0.25(5)	–	42(2)	101
2^{nd} (P)		0.276(5)	0.853(5)	1.69(5)	–	12(2)	
FeSe	102	0.298(5)	0.549(5)	0.29(5)	–	43(2)	
2^{nd} (P)		0.298(5)	0.884(5)	1.61(5)	–	4(2)	
2^{nd} (M)		0.517(9)	0.90(9)	0.19(9)	12.3(7)	10(2)	
FeSe	98	0.311(5)	0.551(5)	0.30(5)	–	42(2)	
2^{nd} (P)		–	–	–	–		
2^{nd} (M)		0.811(7)	0.90(5)	0.08(8)	11.9(9)	13(2)	
$FeSe_{0.75}$							
FeSe	298	0.301(5)	0.495(5)	0.25(5)	–	53(2)	101.5
2^{nd} (P)		0.301(5)	0.886(5)	1.71(5)	–	18(2)	
FeSe	102	0.291(5)	0.555(5)	0.28(5)	–	50(2)	
2^{nd} (P)		0.291(5)	0.982(5)	1.71(5)	–	8(2)	
2^{nd} (M)		0.605(9)	0.812(7)	0.056(9)	10.1(8)	10(2)	
FeSe	101	0.298(5)	0.548(5)	0.29(5)	–	49(2)	
2^{nd} (M)		1.03(9)	0.841(9)	−0.27(7)	9.8(9)	23(2)	
$FeSe_{0.82}$							
FeSe	298	0.361(5)	0.491(5)	0.24(5)	–	64(2)	103
2^{nd} (P)		0.361(5)	0.901(5)	1.72(5)	–	15(2)	
FeSe	104	0.316(5)	0.548(5)	0.29(5)	–	63(2)	
2^{nd} (P)		0.316(5)	0.951(5)	1.80(5)	–	14(2)	
FeSe	102	0.299(5)	0.541(5)	0.291(5)	–	56(2)	
2^{nd} (M)		0.697(8)	0.955(9)	0.12(9)	7.5(9)	17(2)	
$FeSe_{0.9}$							
FeSe	298	0.278(5)	0.445(5)	0.25(5)	–	67(2)	104
2^{nd} (P)		0.278(5)	0.851(5)	1.71(5)	–	17(2)	
FeSe	106	0.291(5)	0.547(5)	0.29(5)	–	63(2)	
2^{nd} (P)		0.291(5)	0.957(5)	1.74(5)	–	18(2)	
FeSe	102	0.290(5)	0.551(5)	0.29(5)	–	63(2)	
2^{nd} (P)		0.290(5)	0.953(5)	1.76(5)	–	6(2)	
2^{nd} (M)		0.688(9)	0.719(9)	0.063(8)	10.7(7)	16(2)	
FeSe	77	0.323(5)	0.554(5)	0.30(5)	–	62(2)	
2^{nd} (M)		0.441(7)	0.935(7)	0.058(9)	16.3(8)	21(2)	

1 Metallic Fe portions of ∼33 %, ∼17 %, ∼12 % and ∼3 % at all indicated temperatures were found for samples with $x = 0.4$, 0.25. 0.18 and 0.1, respectively. Fe_7Se_8 portions of ∼12 %, ∼13 %, ∼16 % and ∼14 % at all indicated temperatures were found for samples with $x = 0.4$, 0.25. 0.18 and 0.1, respectively

FeSe, Fe_7Se_8 and Fe. This was done with the programs integrated in the FullProf software package [11]. A good match was found using an orthorhombic system with lattice parameters a ≈ 8.52 Å, b ≈ 6.96 Å, and c ≈ 4.90 Å(in Pmmm), covering even the tiniest reflections

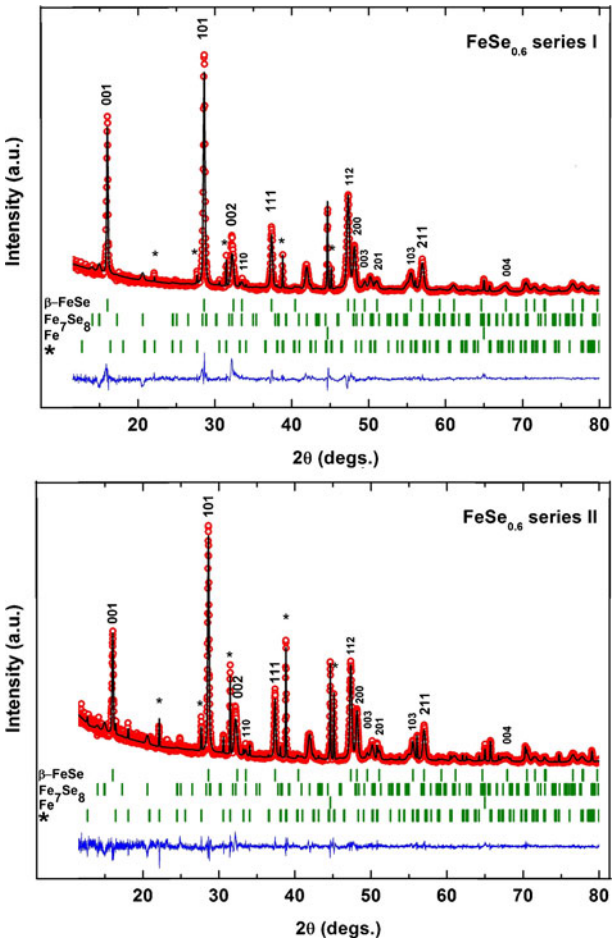

Fig. 2 X-ray powder diffraction patterns for series I and series II $FeSe_{0.6}$ samples. Main peaks of the secondary phase component are denoted by *asterisks*. Indices concern the main β-FeSe phase

left in the XRD pattern. This unit cell is included as a Le Bail fit in the Rietveld refinements shown in Figs. 2 and 3.

Based on the refinements, the ratio of the known components β-FeSe, Fe_7Se_8 and Fe is 9.4:1.4:1 and 3.5:0.8:1 for $FeSe_{0.9}$ and $FeSe_{0.6}$, respectively. The amount of the unknown phase cannot be determined without knowing the crystal structure but by comparing intensities, it can be said that $FeSe_{0.6}$ and $FeSe_{0.9}$ both contain substantial amount of the secondary phase after the second sintering.

These additional XRD peaks were observed also for FeSe single crystals that were grown using the Bridgman method with controlled cooling rate [12], but the phase that gives rise to these peaks was not determined. Upon examining the powder XRD data of the original work [1] it becomes evident that the secondary phase was encountered but left unidentified by the authors.

Mössbauer spectra obtained from samples of series I exhibit only the paramagnetic doublet of the main phase and magnetic Fe_7Se_8 and elementary iron as impurities, with the

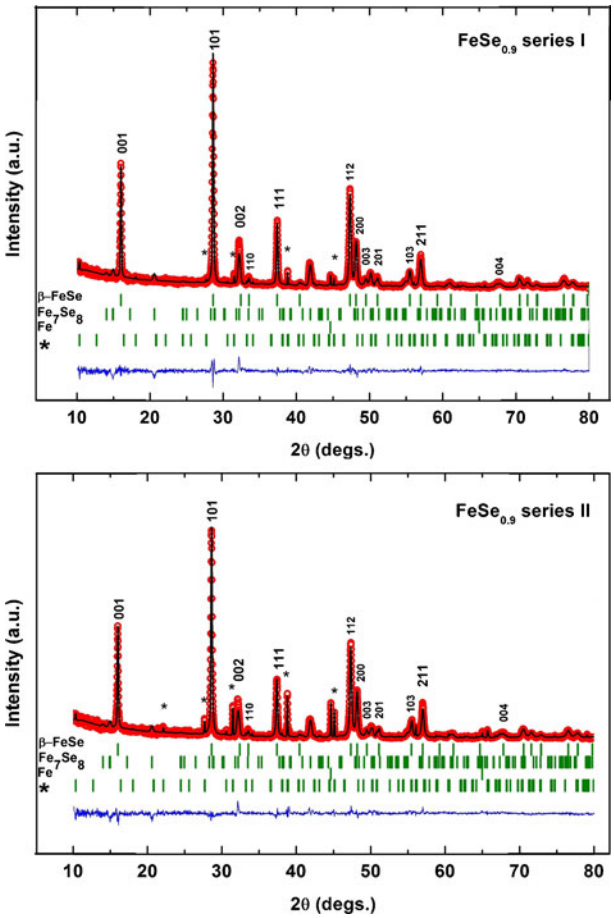

Fig. 3 X-ray powder diffraction patterns for series I and series II $FeSe_{0.9}$ samples. Main peaks of the secondary phase component are denoted by *asterisks*. Indices concern the main β-FeSe phase

secondary FeSe phase barely exceeding the detection limit. The Mössbauer spectra of all investigated samples of series II show the presence of the secondary phase doublet at room temperature, some quantities of Fe_7Se_8 and metallic Fe, Fig. 4. The hyperfine parameters of the main FeSe component and for the secondary phase are given in Table 1. For Fe_7Se_8 literature values of the hyperfine parameters for the corresponding temperatures, quite complex with 3 magnetic subspectra [13], were used. Volume fraction for all components are presented in Table 1.

The main phase has a paramagnetic doublet with $\delta = 0.44$ mm/s and $eQV_{zz}/2 \approx 0.25$ mm/s at room temperature. These parameter values coincide with β-FeSe which has a tetragonal structure and the isomer shift indicates a low-spin state of divalent iron in this material [14]. For the secondary component the isomer shift ($\delta = 0.85$ mm/s) indicates Fe^{2+} in a high-spin state in agreement with earlier data for a similar compound [9]. Presence of interstitial iron a singlet corresponding to trivalent Fe [15] was not observed in the present Mössbauer data. From measurements of Fe(Te,Se) it is known that such Fe species strongly overlap with the percentage main component. Analysis

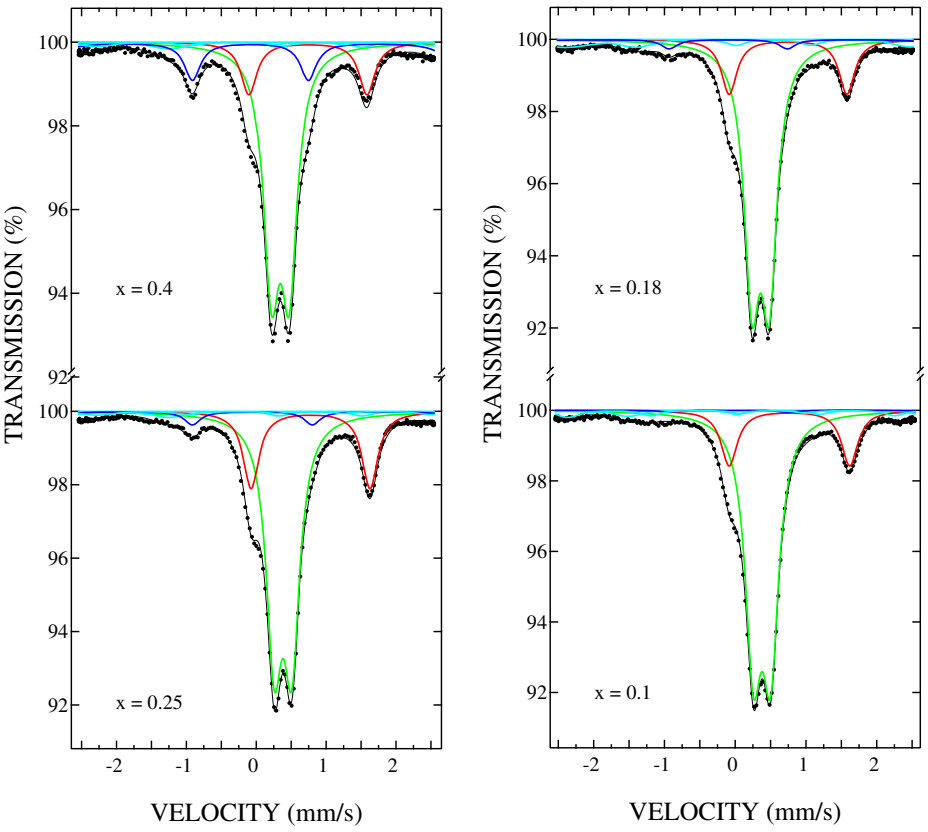

Fig. 4 Mössbauer spectra of $FeSe_{1-x}$ ($x = 0.4, 0.25, 0.18, 0.1$) series II samples at room temperature. *Green*, *blue* and *red lines* indicate the main paramagnetic doublet, elementary iron and secondary phase, respectively. *Lines* (cyan) due to magnetic Fe_7Se_8 are visible in the background

of the XRD data suggests that the possible concentration of interstitial Fe is below a few percents.

The volume fraction of the secondary component depends on the selenium content in the $FeSe_{1-x}$ spectra, Fig. 4. The $FeSe_{0.75}$ compound shows the highest concentration of it, despite the presence of other iron impurities.

The secondary phase undergoes a magnetic transition upon decreasing the temperature. The transition temperature is readily observed in Mössbauer spectra recorded with a temperature step of 0.5 - 1 K, Fig. 5. Similar results were obtained for all investigated samples. For $x = 0.1$ a transition temperature of $\sim$105 K was detected. The transition temperatures for the series II samples are given in Table 1.

From the Mössbauer spectra recorded above and around transition temperature of the secondary phase no changes are observed for the component from the main phase. This also indicates that the main phase and the secondary phase in investigated samples are well separated.

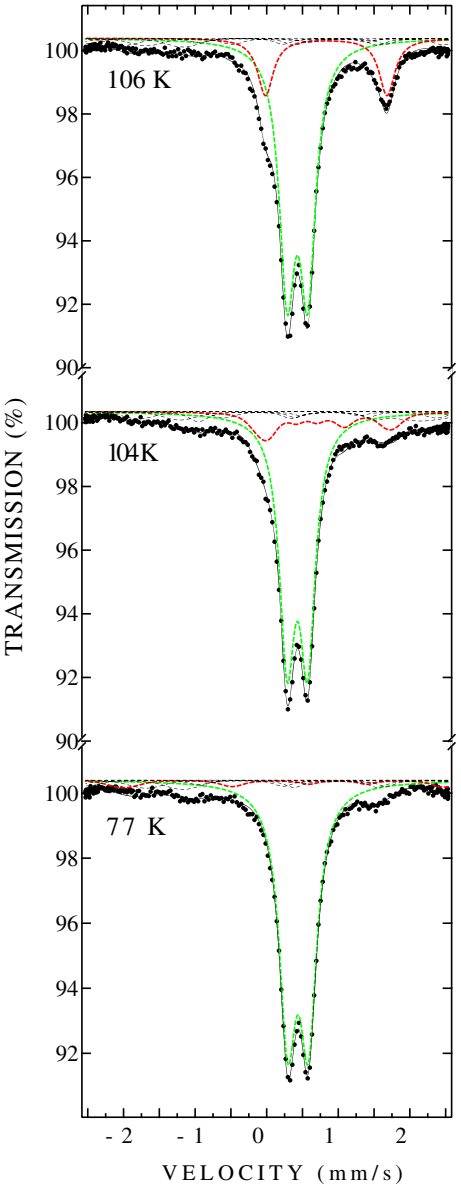

Fig. 5 Mössbauer spectra of the $FeSe_{0.9}$ series II sample recorded at temperatures around the magnetic transition temperature of the secondary phase Fe. *Green* and *red lines* are due to the main phase and secondary phase, respectively. *Weak lines* due to metallic Fe and magnetic Fe_7Se_8 are visible in the background

4 Conclusions

The synthesis conditions for promoting the concentration of a secondary Fe-Se phase in β-FeSe were optimized. A two-step solid-state reaction at 750 °C gives the highest volume fraction of this secondary phase. Mössbauer spectra for all samples obtained by the two step synthesis show the presence of the second paramagnetic doublet with a high quadrupole splitting ($\sim$1.7 mm/s), assigned to the emerging phase. Mössbauer spectra of samples obtained using only one synthesis step did not exhibit the secondary component.

The presence of the secondary phase in the samples after two synthesis was also confirmed by XRD measurements. Secondary phase Fe has valence 2+ and a high-spin state while the main phase Fe atoms are in a divalent low-spin state. The secondary phase Fe atoms undergo a magnetic transition at ∼104 K and the behavior of the Mössbauer spectra recorded at this transition region indicate a spatial separation of the main phase and the secondary phase atoms. Determination of space group and exact stoichiometry of the secondary phase requires further studies.

References

1. Hsu, F.-C., Luo, J.-Y., Yeh, K.-W., Chen, T.-K., Huang, T.-W., Wu, P.M., Lee, Y.-C., Huang, Y.-L., Chu, Y.-Y., Yan, D.-C., Wu, M.-K.: Proc. Natl. Acad. Sci. U.S.A. **105**, 14262 (2008)
2. Imai, T., Ahilan, K., Ning, F.L., McQueen, T.M., Cava, R.J.: PRL **102**, 177005 (2009)
3. Medvedev, S., McQueen, T.M., Troyan, I.A., Palasyuk, T., Eremets, M.I., Cava, R.J., Naghavi, S., Casper, F., Ksenofontov, V., Wortmann, G., Felser, C.: Nat. Mater. **8**, 630 (2009)
4. de Souza, M., Haghighirad, A.-A., Tutsch, U., Assmus, W., Lang, M.: Eur. Phys. J. B **77**, 101 (2010)
5. McQueen, T.M., Huang, Q., Ksenofontov, V., Felser, C., Xu, Q., Zandbergen, H., Hor, Y.S., Allred, J., Williams, A.J., Qu, D., Checkelsky, J., Ong, N.P., Cava, R.J.: Phys. Rev. B **79**, 014522 (2009)
6. Bendele, M., Amato, A., Conder, K., Elender, M., Keller, H., Klauss, H.-H., Luetkens, H., Pomjakushina, E., Raselli, A., Khasanov, R.: PRL **104**, 087003 (2010)
7. Grechnev, G.E., Panfilov, A.S., Desnenko, V.A., Fedorchenko, A.V., Gnatchenko, S.L., Chareev, D.A., Volkova, O.S., Vasiliev, A.N.: J. Phys. Condens. Matter. **25**, 046004 (2013)
8. Libäck, J.-P.: Master's Thesis, Åbo Akademi (2010)
9. Hamdeh, H.H., El-Tabey, M.M., Asmatulu, R., Ho, J.C., Huang, T.W., Yeh, K.W., Wu, M.K.: Eur. Phys. Lett. **89**, 67009 (2010)
10. Pimentel Jr, J.L., Serbena, F.C., Jurelo, A.R.: J. Supercond. Nov. Magn. **24**, 1437 (2011)
11. Rodriquez-Carvajal, J.: Physica B **192**, 55 (1993)
12. Yang, C.-M., Chen, P.-W., Kou, J.-C., Diko, P., Chen, I.-G., Wu, M.-K.: IEEE Trans. Appl. Supercond. **21**, 2845 (2011)
13. Ok, H.N., Lee, S.W.: Phys. Rev. B **8**, 4267 (1973)
14. Lindén, J., Rautama, E.-L., Karppinen, M., Yamauchi, H.: Hyperfine Interact. **208**, 133 (2012)
15. Błachowski, A., Ruebenbauer, K., Zajdel, P., Rodriques, E.E., Green, M.A.: J. Phys. Condens. Matter **24**, 386006 (2012)